Coastal ocean and shelf-sea biogeochemical cycling of trace elements and isotopes: lessons learned from GEOTRACES

Matthew A. Charette[*a], Phoebe J. Lam[b], Maeve C. Lohan[c], Eun Young Kwon[d], Vanessa Hatje[e], Catherine Jeandel[f], Alan M. Shiller[g], Gregory A. Cutter[h], Alex Thomas[i], Philip W. Boyd[j], William B. Homoky[k], Angela Milne[l], Helmuth Thomas[m], Per S. Andersson[n], Don Porcelli[o], Takahiro Tanaka[p], Walter Geibert[q], Frank Dehairs[r], Jordi Garcia-Orellana[s]

*corresponding author, mcharette@whoi.edu

[a]Department of Marine Chemistry and Geochemistry, Woods Hole Oceanographic Institution, Woods Hole, MA 02543 USA

[b]Department of Ocean Sciences, University of California-Santa Cruz, Santa Cruz, CA 95064 USA

[c]Ocean and Earth Science, National Oceanography Centre, University of Southampton, Southampton SO14 3ZH, United Kingdom

[d]Research Institute of Oceanography, Seoul National University, Seoul 151-742 Korea

[e]Centro Interdisciplinar de Energia e Ambiente, Inst. de Química, Universidade Federal da Bahia, Salvador, 40170-115 Brazil

[f]LEGOS (CNRS/CNES/IRD/UPS), Observatoire Midi-Pyrénées, Toulouse, 31400, France

[g]Department of Marine Science, University of Southern Mississippi, Stennis Space Center, MS 39529 USA

[h]Department of Ocean, Earth, and Atmospheric Sciences, Old Dominion University, Norfolk, VA 23529 USA

[i]School of GeoSciences, University of Edinburgh, Edinburgh, EH9 3FE, United Kingdom

[j]Institute of Marine and Antarctic Studies, University of Tasmania, Hobart, Tasmania, 7005 Australia

[k]Department of Earth Sciences, University of Oxford, Oxford, OX1 3AN, United Kingdom

[l]School of Geography, Earth and Environmental Sciences, Plymouth University, Plymouth, PL4 8AA, United Kingdom

[m]Department of Oceanography, Dalhousie University, Halifax, NS, B3H 4R2 Canada

[n]Department of Geosciences, Swedish Museum of Natural History, Stockholm SE-104 05, Sweden

[o]Department of Earth Sciences, University of Oxford, Oxford OX1 3AN, United Kingdom

[p]Atmosphere and Ocean Research Institute, University of Tokyo Kashiwanoha 5-1-5 Kashiwa Chiba, 277-8564, Japan

[q]Marine Geochemistry Department, Alfred Wegener Institute Helmholtz Centre for Polar and Marine Research, Am Handelshafen 12, 27570 Bremerhaven, Germany

[r]Earth System Sciences & Analytical, Environmental and Geo-Chemistry, Vrije Universiteit Brussel, Brussels, B-1050 Belgium

[s]Physics Department-ICTA, Universitat Autònoma de Barcelona, Barcelona, 08193 Spain

Abstract

Continental shelves and shelf seas play a central role in the global carbon cycle. However, their importance with respect to trace element and isotope (TEI) inputs to ocean basins is less well understood. Here, we present major findings on shelf TEI biogeochemistry from the GEOTRACES program as well as a proof-of-concept for a new method to estimate shelf TEI fluxes. The case studies focus on advances in our understanding of TEI cycling in the Arctic, transformations within a major river estuary (Amazon), shelf sediment micronutrient fluxes, and basin-scale estimates of submarine groundwater discharge. The proposed shelf flux tracer is 228-radium ($T_{1/2}$=5.75 y), which is continuously supplied to the shelf from coastal aquifers, sediment porewater exchange, and rivers. Model-derived shelf ^{228}Ra fluxes are combined with TEI/ ^{228}Ra ratios to quantify ocean TEI fluxes from the western North Atlantic margin. The results from this new approach agree well with previous estimates for shelf Co, Fe, Mn, and Zn inputs and exceed published estimates of atmospheric deposition by factors of ~3-23. Lastly, recommendations are made for additional GEOTRACES process studies and coastal margin-focused section cruises

86 that will help refine the model and provide better insight on the mechanisms driving
87 shelf-derived TEI fluxes to the ocean.
88
89 **1. Introduction**
90 Continental shelves and shelf seas play an important role in modulating the transfer
91 of materials between the land and ocean. As such, quantifying processes occurring
92 within this key interface is essential to our understanding of the biogeochemistry of
93 trace elements and their isotopes (TEIs) in the ocean, a major goal of the
94 GEOTRACES program (www.geotraces.org). Moreover, the supply and removal of
95 elements in coastal oceans have direct influence on the structure of ocean
96 ecosystems and their productivity. Although coastal oceans comprise only around
97 7% of the total ocean area, they support 15-20% of total primary productivity and
98 provide 90% of the world's fish yield [1]. As a critical Earth system interface, a large
99 proportion of CO_2 exchange between the ocean and atmosphere occurs over the
100 shelf, which is thought to be a net sink for both atmospheric and terrestrial carbon
101 [2-4].
102
103 In the nearshore environment, estuaries are known to be important zones of TEI
104 processing [5]. One classic example is the removal of dissolved iron during estuarine
105 mixing, which has been shown in many cases to vastly diminish the riverine flux of
106 this element to the ocean [6-8]. Similarly, uranium has an active biogeochemistry in
107 estuaries and salt marshes, which generally, yet not exclusively, act as sinks for
108 dissolved U [9-11]. Dissolved organic matter (DOM) and several other trace
109 elements may also be removed, at different rates, along the salinity gradient of
110 estuaries and shelves [8, 12-15], while some TEIs like barium and radium are
111 known to be added due to desorption from riverine particles [16-20]. In addition to
112 rivers [21], submarine groundwater discharge (SGD) may represent a large source
113 of TEIs to the coastal ocean [22, 23]. Comprising a mixture of meteoric groundwater
114 and seawater circulated through coastal aquifers, SGD has been estimated to exceed
115 river discharge both regionally [24, 25] and by a factor of 3-4 on a global basis [26].
116 Furthermore, SGD has been shown to be an important source of micronutrients (e.g.

Fe [27]), contaminants (e.g. Hg [28] and Pb, [29]), and TEIs commonly used as paleo-tracers (e.g. U and Ba [30]).

For some elements, boundary exchange processes involving sedimentary deposits on the continental margins may have substantial or even greater fluxes to the ocean than rivers. Diffusive benthic fluxes can be a major source of dissolved rare earth elements (REE) to the ocean at levels that could explain the missing source observed in recent isotopic modeling studies [31-33], where the REE flux from shelf sediments is larger than other REE sources to the ocean [34]. The sedimentary remobilization of Nd along continental margins, specifically due to sediment dissolution, also illustrates the importance of shelf porewater exchange processes as a source of TEIs to the ocean [31]. Studies at "mid-ocean" shelves, such as the Kerguelen and Crozet Plateaus, showed a substantial role of sedimentary iron release in alleviating Fe limitation and enhancing carbon sequestration in the Southern Ocean [35-37].

The GEOTRACES program has carried out basin scale sections to quantify and identify the processes that supply TEIs at ocean boundaries (atmosphere-ocean, sediment-water, ocean crust-overlying water, continent-ocean [38-41]). However, the coastal or shelf ocean is an interface that requires additional process studies to investigate the key processes impacting on the biogeochemical cycles of TEIs. The identification and quantification of TEI distributions and fluxes along ocean margins are important for a number of reasons, including their sensitivity to changing precipitation and wind patterns, and potential impacts on aquaculture and fisheries. Particularly striking is the extent and rate at which humans have modified the coastal zone worldwide [42], a narrow strip of land within 100 km of the ocean where half of the world's population lives and where three-quarters of all large cities are located [43, 44]. The impacts are numerous and include large-scale bottom water anoxia, eutrophication, acidification, overfishing and anthropogenic contaminant inputs. For instance, global budgets of TEIs such as Pb and Hg have already been significantly altered in the ocean as a result of human induced

activities such as acid mine drainage [45, 46]. The role of changing sea-ice cover may affect shelf TEI transport rates, and TEI discharges associated with the accelerated melting of large ice sheets have the potential to increase in magnitude over the coming decades to centuries. For present-day Greenland, the Fe flux may already be on par with the total amount of Fe delivered to the North Atlantic Ocean via dust [47], but the scale of this impact depends on the quantification of fluxes between the coast and open ocean [48].

An understanding of the mechanisms governing the linkages between the terrestrial→shelf→open ocean continuum is crucial [49]. Although some GEOTRACES process studies have focused more in near shelf regions, GEOTRACES sections to date have, by design, focused primarily on open ocean transects. Here we highlight several examples of where GEOTRACES studies have yielded significant insight on shelf TEI processes, defined as those occurring along ocean margins at water depths <200 m. We further propose a new approach for quantifying the shelf flux of TEIs using a radium isotope tracer (^{228}Ra) and inverse modeling techniques. Finally, we recommend a series of efforts that are necessary to constrain the exchange processes at coastal/shelf ocean interfaces and to aid in the prediction of fluxes of TEIs from this boundary to the ocean.

2. Significant GEOTRACES contributions to our understanding of shelf impacts on TEI budgets for the open ocean

2.1 The Arctic

The Arctic Ocean is unique among the major ocean basins in having as much as one half of its area taken up by shelves [50]. Further, the basin receives a disproportionate percentage of the world's river discharge (10% [51]). Arctic waters are also highly stratified, with a distinct low salinity surface mixed layer, a strong halocline, and clear shelf and river inputs. Because of these features, the impact of shelf-basin interactions on TEI distributions is particularly prominent throughout the Arctic Ocean. However, TEI data have been limited due to the logistical difficulties of reaching remote and ice-covered regions. The International

Polar Year 2007-2008 provided a launching pad for the GEOTRACES program, with five cruises in the Arctic region between 2006-2009, which led to new insights about important Arctic coastal processes acting on TEI distributions. More recently, in summer 2015 three nations mounted full GEOTRACES Arctic cruises; the results of that coordinated effort are forthcoming.

High concentrations of shelf-derived trace metals in surface waters of the central Arctic were reported by Moore [52]. This included Cd, which has been found to exhibit only minor isotope shifts compared to other ocean basins where greater variations are generated through biological removal [53]. Data from the Swedish-Russian GEOTRACES (GIPY13) cruise to the Siberian shelves found that Cd was not removed in the Lena estuary, and there were further Cd additions to shelf waters from the shelf sediments [54]. Another example of shelf influence on the deep basin is the distribution of Ba, which is strongly enriched in estuarine waters due to desorption from river sediments. In theory, Ba distributions can delineate shelf TEI sources; however, isolating the terrestrial Ba source may be complicated due to biogenic Ba uptake and vertical redistribution [55]. As part of the Canadian IPY-GEOTRACES, a dissolved Ba cross-section through the Canadian Archipelago revealed high surface water Ba concentrations near the Horton River and a pronounced Ba maximum in the upper halocline waters (Fig. 1; [56]). The latter was thought to be due in part to Ba released to subsurface waters in the wake of organic matter remineralization, a finding similar to Roeske et al. [55] who reported that remineralization from the Siberian shelf led to a similar Ba enrichment below the surface mixed layer. This may represent a dynamic process that is not at steady-state: such 'metabolic Ba' concentrations in the subsurface layer increase with the arrival of organic matter sometime after the spring bloom, approaching maximum values toward the end of winter [56].

A strong Mn enrichment was also found in the surface layer of the central basin due to riverine inputs of Mn (Fig. 2; [57]), though the inferred river component indicated that river waters were significantly depleted by estuarine processes. Mid-depth

enrichments of Mn on the shelf also suggested that there were benthic contributions, though this sediment source did not extend a significant distance off-shelf. The first measurements of Ga in Arctic waters found that its distribution reflected mixing between Atlantic and Pacific waters, with evidence of both riverine input and scavenging removal in shelf waters of the Beaufort Sea [58]. Further studies of the shelf cycling of Ga and related elements (especially Al, which is chemically similar to Ga though more readily scavenged) could provide insights into how shelf scavenging removal affects the off-shelf transport of reactive TEIs.

Isotope variations in Nd have been widely used to understand shelf-water interactions and riverine inputs. Within the Arctic Ocean, gradients between surface and halocline waters reflected inputs from the Pacific [59] as well as a source that isotopically matched the major rivers, indicating that the concentrations of the river components reaching the central basin did not reflect the considerable estuarine Nd losses commonly seen elsewhere [60]. These datasets were extended with samples from the BERINGIA 2005 and GIPY13 GEOTRACES cruises, which clearly demonstrated how Nd isotopes and concentrations in the Pacific layer were modified while crossing the Bering Sea through sediment-water exchange processes as was inferred for other shelf areas (Fig. 3; [61]). Furthermore, Lena River waters did not suffer strong modification through estuarine losses like in the Amazon [62].

Data from GEOTRACES cruises have also documented the behavior of carbon on the Arctic shelves. Alling et al. [63] demonstrated for the first time that substantial degradation of DOC occurs in the Lena River estuary, with greater degradation in the broad East Siberian Seas where shelf water residence times are several years; along with degassing of CO_2, this process was clearly shown in DIC $\delta^{13}C$ signatures [64]. Rising Arctic Ocean temperatures are leading to the thawing of permafrost and release of its stored methane [65, 66]. Indeed, preliminary results from the recent 2015 U.S. GEOTRACES Arctic section (GN01) show shelf enrichments of tracers such as CH_4 [67], though the impact of this process on other TEIs remains to be seen.

Essential to addressing these and other questions, are radioactive TEIs, which allow for quantification of the time scales associated with these shelf-basin exchange processes, as has been demonstrated by Rutgers van der Loeff et al. [68] for ^{228}Ra and more recently by Rutgers van der Loeff et al. [69], who used the ^{228}Th/^{228}Ra daughter/parent ratio, which is depleted on the shelves but climbs in the particle-depleted central basin, to estimate an age of 3 years for waters at the Gakkel Ridge.

2.2 The influence of major rivers

River-dominated shelves have the potential to be important point sources for TEI delivery to marginal seas and their adjacent ocean basins. For example, Nd isotopic compositions have been measured together with dissolved and colloidal REE concentrations and radium isotope activities in the Amazon estuary salinity gradient as part of the GEOTRACES process study AMANDES (Fig. 4; [13]). The sharp drop in REE concentrations in the low-salinity region was driven by the coagulation of colloidal material. At mid salinities, dissolved REE concentrations increased, a result of REE release from lithogenic material, a conclusion supported by the Nd isotopic signature within the estuary. Concurrent measurements of the short-lived Ra isotopes (^{223}Ra, $t_{1/2}$=11.4 d and ^{224}Ra, $t_{1/2}$=3.7 d) revealed that this dissolution process is rapid, on the time scale of 3 weeks. These findings have significant implications for the global marine Nd budget and other TEIs that undergo similar sediment-water exchange processes. This study reinforces one of the original concepts of the GEOTRACES program: the power of synoptic and multiple TEI sampling approaches to understanding ocean biogeochemical cycling.

2.3 Evidence for eddy-mediated cross-shelf transport of iron

Although dust deposition is considered the dominant source of iron to the open ocean, it has now been well established that long-range transport of shelf Fe in high nutrient low chlorophyll (HNLC) regions are a factor in the development of blooms 100's to 1000's of kilometers offshore (e.g. [37, 70-72]) and can dominate iron supply on the global scale [73]. While radium isotopes have been used to quantify this source [74-76], isolating the shelf source on basin-scales is not easily

accomplished in regions beyond the Southern Ocean where other inputs (e.g. dust, hydrothermal vents) may be co-occurring. A 2008 GEOTRACES process study, 'FeCycle', focused on biogeochemical cycling within an eddy off the eastern seaboard of the north island of New Zealand, which is seasonally oligotrophic and has spring diatom blooms [77]. The study revealed that the iron supply for these blooms comes from cross shelf transport of metals that are likely 'picked up' on the shelf and moved offshore in an eddy. This conclusion was reached based on high dissolved and particulate Mn within the eddy and from trajectory analysis using a satellite altimetry model (Fig. 5).

2.4 Apportioning sources of iron using iron isotopes

In addition to transport models, isotopes of iron have recently been used as tracers of oceanic Fe sources [78-81]. Novel high throughput methods [82] have enabled high-resolution sampling on ocean section cruises like GEOTRACES. Recently, Conway and John [83] used this approach to apportion iron sources to the North Atlantic according to dust input, hydrothermal venting, and two types of sediment fluxes: reductive and non-reductive sedimentary release. While they estimated that dust was the dominant Fe source, they reported that non-reductive release from sediments on the North American margin was a major local source that contributed between 10-19% of the iron basin-wide (Fig. 6). In addition, Fitzsimmons et al. [84] reported that ~60-80% of the dissolved Fe in this region was in the colloidal phase, which has implications for the bioavailability and long-range transport of this important micronutrient. At the African margin, reductive dissolution in sediments accounted for 1-4% of the iron basin-wide [83]. Further south, Homoky et al. [85] attributed a high-proportion of dissolved Fe present in margin sediments to non-reductive release, and earlier studies of pore waters that were rich in colloidal iron had similar isotope compositions [86, 87], which supports the view that colloids may influence the stability and transport of iron from non-reductive sediment sources in ocean basins [88].

2.5 Time variations in basin-scale submarine groundwater discharge

Submarine groundwater discharge has received increased attention over the past two decades as a source of TEIs to the ocean. The majority of the early studies focused on the local scale, though Moore et al. [24] was able to estimate SGD to the Atlantic Ocean using ^{228}Ra ($T_{1/2}$=5.75 y) inventories from the Transient Tracers in the Ocean (TTO) program, and determined that the SGD flux was 2–4x10^{13} m^3/y, equivalent to 80-160% of the freshwater discharge from rivers. Since the TTO data had been collected in the 1980s, the Atlantic Ocean ^{228}Ra inventory had largely decayed and been replaced by the time of the 2010-11 U.S. GEOTRACES North Atlantic program. This afforded Charette et al. [89] the opportunity to evaluate whether or not this ocean basin was in steady-state with respect to SGD inputs. Using ^{228}Ra data collected along transects between North America and West Africa, and Western Europe and West Africa, they observed essentially no change in the upper ocean inventory of this tracer, suggesting that SGD had not changed despite significant changes in groundwater withdrawals during the intervening period.

Kwon et al. [26] took this a step further and used inverse modeling techniques applied to a global ^{228}Ra dataset to calculate total SGD to the ocean. This approach yields the total ^{228}Ra flux from the shelf, which in addition to the SGD input includes the riverine discharge and shelf sediment diffusive sources. Sediments of continental shelves and aquifers are important areas for in situ production of Ra isotopes through continuous decay of their parent thorium isotopes (e.g. Moore et al. [90], while rivers supply dissolved Ra isotopes as well as Ra sourced from desorption from suspended sediments in the estuarine mixing zone [91]. For a number of TEIs, estimates for riverine inputs are generally well constrained, however, due to estuarine processing and direct TEI inputs to the shelf we lack a method or approach for quantifying the net flux of TEIs across the interface between coastal and open ocean waters.

2.6 ^{228}Ra as a shelf TEI flux gauge

To this end we are proposing an approach for quantifying shelf TEI fluxes that utilizes ^{228}Ra as a shelf flux gauge. This method takes advantage of the global inverse

model of Kwon et al. [26], which focused on isolating the flux ^{228}Ra via SGD to the ocean, but at its root is designed to estimate the total ^{228}Ra flux from all shelf sources required to balance the upper ocean ^{228}Ra inventory and decay. Because of its strong shelf source and relatively short half life (on the time scale of mixing), the majority of the upper 1000 m ^{228}Ra inventory in the basin can be traced back to the shelf. This inverse approach to estimating shelf ^{228}Ra flux has the advantage of integrating the shelf source of ^{228}Ra over annual to decadal timescales, which averages out seasonal variability that hampers the use of nearshore ^{228}Ra gradients to estimate shelf ^{228}Ra fluxes directly [92]. As a first order estimate, we propose to use the ratio of nearshore gradients of dissolved TEI and ^{228}Ra measured over the shelf and nearby stations during specific GEOTRACES cruises to link the model-derived shelf-ocean ^{228}Ra flux to shelf-ocean TEI fluxes.

The full details of the global ^{228}Ra model can be found in Kwon et al. [26]. Briefly, the model employs a 2°x2° global circulation model where the domain is restricted to between 60°S and 70°N due to insufficient ^{228}Ra coverage in the polar oceans. The vertical resolution is fine near the surface (~40 m) and coarse near the ocean bottom (~600 m). The coastal ^{228}Ra source is defined as that originating from the ocean grid boxes adjacent to land boxes with a depth of less than ~200 m. The coastal source is optimized through a minimization scheme whereby the reported fluxes are those that result in the best fit between the model and observed ^{228}Ra activities in the basin. The total ^{228}Ra fluxes for each 2°x2° margin grid cell are shown in Figure 7a. The highest total margin inputs are to the North Pacific and Indian Ocean basins. For both the Atlantic and Pacific Oceans, the western margin ^{228}Ra fluxes exceed those from the east, likely due to a combination of major river inputs, SGD, and the presence of broad continental margins and/or extensive shelf seas. The relatively narrow shelf along the North American active margin in the Pacific appears to have the lowest inputs on average.

Assuming shelf-ocean exchange is primarily driven by eddy diffusion, the net cross-shelf TEI flux can be linearly scaled with the net cross-shelf ^{228}Ra flux as follows:

$$\text{TEI } flux = {}^{228}\text{Ra } flux \times \left(\frac{\Delta \text{TEI}}{\Delta {}^{228}\text{Ra}}\right) = {}^{228}\text{Ra } flux \times \left(\frac{\text{TEI}_{\text{shelf}} - \text{TEI}_{\text{ocean}}}{{}^{228}\text{Ra}_{\text{shelf}} - {}^{228}\text{Ra}_{\text{ocean}}}\right) \quad (1)$$

where $\text{TEI}_{\text{shelf}}$ and ${}^{228}\text{Ra}_{\text{shelf}}$ are the average concentrations of the TEI of interest and ^{228}Ra over the shelf water column (<200 m). The $\text{TEI}_{\text{ocean}}$ and ${}^{228}\text{Ra}_{\text{ocean}}$ are the average dissolved TEI and ^{228}Ra in the open ocean (<200 m) (see supplementary material). For highly reactive elements with very low open ocean concentrations, this ratio may be close to ($\text{TEI}_{\text{shelf}}$ /${}^{228}\text{Ra}_{\text{shelf}}$). However, for this approach to be applicable to TEIs with a wide range of particle reactivities, including those with non-negligible open ocean concentrations relative to shelf concentrations, $\Delta\text{TEI}/\Delta{}^{228}$Ra should be employed. For shelves where the net cross-shelf advective flux is substantial, the TEI flux would not scale linearly with ^{228}Ra flux as illustrated in the supplementary materials.

It is important to recognize that fluxes derived from this approach are the net dissolved TEI input rate to the ocean at the shelf break (200 m). Hence, the flux at this boundary is not necessarily what might be expected to reach the ocean interior due to the varying degrees of TEI particle reactivity and biological cycling. Further, the method in theory should account for any TEI removal over the shelf; therefore, fluxes may not equal the sum of the inputs along the boundary (e.g. rivers, SGD, sediment diffusion). Finally, we note that many of the TEI shelf input and removal processes vary seasonally, not necessarily in concert with seasonal variability in ^{228}Ra sources, and that not all shelf sources are expected to have uniform $\Delta\text{TEI}/\Delta{}^{228}$Ra. For example, sporadic sources due to rivers and SGD may hinder a proper averaging of $\Delta\text{TEI}/\Delta{}^{228}$Ra over large shelf areas. While the spatial and temporal variability in a particular $\Delta\text{TEI}/\Delta{}^{228}$Ra must be fully assessed before this method is to be widely employed, we hope that this exercise provides a first order assessment of the importance of shelf TEI fluxes to the ocean in comparison to other external sources.

For the purpose of this exercise, we chose to focus on the North Atlantic Ocean basin due to the availability of synoptic TEI and ^{228}Ra data from the U.S. GEOTRACES GA03

394 cruises, though the scope could be expanded as more GEOTRACES datasets become
395 available. These cruises crossed or approached three main shelf areas: the
396 Northwest Atlantic shelf south of Woods Hole, MA (USA), the Iberian margin, and
397 the Mauritanian upwelling zone off of Western Africa. For perspective, the combined
398 North Atlantic shelf ^{228}Ra flux (23.9 ± 4.6 x 10^{22} atoms/y) accounts for
399 approximately 25% of the global shelf flux (96 ± 5 x 10^{22} atoms/y; Fig. 7a; [26]). Of
400 the three GA03 cruise shelf crossings, however, only the Northwest Atlantic has
401 multiple stations in close proximity to the shelf break and a shelf where elemental
402 transport is dominated by eddy diffusion [93]. As a result, the western North
403 Atlantic shelves (0° -70°N), which are responsible for about 60% of the shelf ^{228}Ra
404 input to this ocean basin (14.3 ± 1.9 x 10^{22} atoms/y), will be the focus of our shelf
405 TEI flux calculations.
406
407 Though there is a long list of TEIs fluxes that could be determined using this
408 method, we chose to focus on four (dissolved Fe, Mn, Co, Zn) that span a range of
409 particle reactivity and play a role in upper ocean biogeochemical cycling. The
410 ΔTEI/Δ^{228}Ra ratios were calculated using equation (1) from averaged concentration
411 data for the two Northwest Atlantic nearshore stations (GA03, KN204-1 stations
412 1,2) and open ocean station 16 (GA03, KN204-1; Fig. 7b).
413
414 By combining the model ^{228}Ra fluxes and ΔTEI/Δ^{228}Ra, we can estimate the annual
415 shelf TEI inputs to the western North Atlantic Ocean (Table 1). The western N.
416 Atlantic shelf Co flux (1.4±0.4x10^{8} mol/y) is consistent with literature estimates
417 from a variety of independent approaches. Saito et al. [94] estimated that the shelf
418 dissolved Co flux for the Peru upwelling region was 2.0x10^{7} mol/y, which compares
419 well with our estimate considering that we integrated over a ~7 times larger area.
420 Lateral shelf area normalized Co fluxes of 6.2-10 μmol m^{-2} y^{-1} were reported by
421 Bown et al. [95] for the S. Atlantic near Cape Town. These are a factor of ~5-10
422 lower than the shelf-normalized fluxes for the western N. Atlantic margin (Table 1;

56 μmol m^{-2} y^{-1}), though their estimate was based on transport across a boundary several hundred km from the shelf-break.

The $\Delta TEI/\Delta^{228}Ra$ approach yielded a shelf Fe flux of $3.9\pm1.4x10^8$ mol/y for the western N. Atlantic. When normalized to shelf-area, this flux is 160 μmol m^{-2} y^{-1}. Sedimentary Fe inputs [88], which are expectedly higher as they do not account for any removal over the shelf, range from 900 μmol m^{-2} y^{-1} [73] to 1570 μmol m^{-2} y^{-1} [71] to 2700 μmol m^{-2} y^{-1} [96]. On a global scale, the shelf-sedimentary Fe inputs as reported by Tagliabue et al. [73], Elrod et al. [71], and Dale et al. [96] are $2.7x10^{10}$ mol/y, $8.9x10^{10}$ mol/y, and $7.2x10^{10}$ mol/y, respectively. The western N. Atlantic Ocean total shelf input as determined by our method would therefore represent only 0.4-1.4% of the global sediment flux. If we assume that our $\Delta Fe/\Delta^{228}Ra$ is comparable to the global shelf average, our approach would predict a global shelf-ocean Fe flux of $2.3x10^9$ mol/y. If the western N. Atlantic shelf is representative of shelf systems globally, our model suggests that only a small fraction of the shelf sedimentary Fe input is exported to the open ocean and therefore available for biological uptake where Fe may be limiting.

The western N. Atlantic Mn shelf flux is $5.4\pm1.0x10^8$ mol/y or 220 μmol m^{-2} y^{-1}. Literature values for shelf Mn fluxes are largely focused on the shelf sediment source. For example, Landing and Bruland [97] reported sedimentary Mn flux of up to 140 μmol m^{-2} y^{-1} for the Monterey Shelf, while McManus et al. [98] observed much higher values for the Oregon/California shelf (2900±900 μmol m^{-2} y^{-1}). The former agrees quite well with our estimate based on equation (1) while the latter is likely higher due to the high productivity associated with the strong upwelling in that region. Lastly, the total Zn shelf flux is $1.6\pm0.6x10^9$ mol/y or 630 μmol m^{-2} y^{-1}. To the best of our knowledge, the shelf Zn flux estimates reported herein are the first of their kind.

In terms of other major sources to the surface ocean, shelf inputs can be on par with or even dominant for certain TEIs. The dissolved cobalt flux for the western N. Atlantic shelf alone is over an order of magnitude higher than the atmospheric deposition of soluble Co to the entire ocean basin as reported by two independent studies (~11×10^6 mol/y; [99, 100]). Soluble Fe (wet+dry) atmospheric deposition to the tropical N. Atlantic ranges from 2.9-43 μmol m^{-2} y^{-1} [101]; scaled to the basin the atmospheric Fe flux becomes 1.2-18×10^8 mol/y or 31-460% of the western North Atlantic dissolved shelf flux using the TEI/^{228}Ra approach. Powell et al. [101] also reported soluble (wet+dry) atmospheric Mn fluxes, which we scaled to the N. Atlantic (0.75-15×10^8 mol/y), equivalent to 14-280% of the shelf inputs reported herein. Assuming 15% solubility, Little et al. [102] estimated the atmospheric Zn input to the surface ocean to be 6.9×10^7 mol/y; our estimates for the western North Atlantic shelf alone exceed that flux by a factor of ~23. Higher concentrations of Zn along with lighter isotopes were observed at both eastern and western Atlantic margins indicating sediments were a source of Zn to this region [83]. Our net shelf-ocean flux of Zn is almost a factor of three higher than the Little et al. [102] *global* estimate for riverine input (5.9×10^8 mol/y); this is in contrast with their suggestion that scavenging removal of Zn and burial in continental margin sediments might represent the "missing sink" for Zn in the global ocean mass balance for this element.

3. Recommendations for the future

We have presented a possible path forward in quantifying TEI shelf-open ocean exchange rates using ^{228}Ra and demonstrated the potential of the method by focusing on the western North Atlantic Ocean. This exercise was made possible by publication of a recent global model for shelf radium inputs and synoptic TEI and ^{228}Ra measurements on a series of U.S. GEOTRACES cruises in 2010-11. Since Ra isotope measurements are not a requirement for GEOTRACES compliance, we suggest that future section cruises and shelf process studies include at least ^{228}Ra so that we can better understand how to relate this tracer to other TEIs. Ra isotope data are especially needed for the Indian and Pacific Oceans where historical data

483 coverage is sparse. Shelf process studies would be needed for a range of shelf
484 settings, i.e. how do $\Delta TEI/\Delta^{228}Ra$ ratios vary seasonally and as a function of
485 hydrological state, shelf width, and coastline lithology (e.g. karst vs. volcanic)?
486 Lastly, for shelf environments where advection plays an important role in TEI
487 transport, a second conservative tracer in addition to ^{228}Ra would be needed to
488 constrain the shelf-ocean TEI flux (Supplementary Material).
489
490 While we have used an inverse approach, which was based on a coarse resolution
491 model, in order to calculate shelf fluxes at a near basin-wide scale, a finer resolution
492 model needs to be combined with coastal ^{228}Ra and TEI data in order to constrain
493 various shelf TEI sources more precisely. Where ^{228}Ra measurements are not
494 possible on future GEOTRACES cruises, we advocate for concurrent physical
495 measurements that may also be used to quantify the shelf flux of TEIs. For example,
496 Tanaka et al. [103] combined DFe distributions with turbulence measurements
497 using a vertical microstructure profiler (VMP) in the Bering Sea; they found that
498 productivity in this region was driven in part by injections of iron-rich subsurface
499 layer at the southeastern shelf break.
500
501 Our discussion above highlights the potential importance of shelf processes on open
502 ocean TEI distributions. Results to date are somewhat limited because of the
503 programmatic emphasis placed on open ocean full depth profiles. For example, lack
504 of data over the shelf for GA03 precluded the inclusion of the eastern boundary
505 shelves in our analysis of TEI fluxes to the North Atlantic Ocean. To better
506 understand the role of shelf input to the open ocean (and vice versa) in global TEI
507 budgets, future GEOTRACES sections may need to be reconfigured with an increased
508 emphasis on shelf stations. Given the shallow depths involved, this change would
509 not impact ship-time requirements to any significant extent. Also, sections in
510 regions with wide shelves and high ratios of shelf area to open water will be
511 particularly useful. The recent 2015 Canadian, U.S., and German sections in the
512 Arctic Ocean are examples of this approach. Fortunately, Ra isotopes were measured
513 on all three cruises.

514

515 There are a number of margin-centric GEOTRACES sections that have been
516 identified in the program planning documents but have yet to be realized due to a
517 variety of factors. These include two of the three proposed for the coastal China
518 seas, Brazil margin, and the Gulf of Mexico. Regarding the latter, the 2007
519 GEOTRACES Atlantic Workshop Report identified a section through the Caribbean
520 and Gulf of Mexico that contains significant opportunities to examine shelf impacts.
521 Roughly a third of the area of the Gulf of Mexico is comprised of shelf waters less
522 than 200 m deep. Portions of the coastline are river dominated (Mississippi) while
523 others are groundwater runoff dominated carbonate platforms (Yucatan peninsula,
524 southern Florida). Furthermore, the Loop Current, a major oceanic current, runs
525 through the Gulf, variably interacting with the shelf. Thus, the Gulf of Mexico is a
526 unique basin for the study of margin/open ocean interactions. Surprisingly, though,
527 despite the significant interest in Louisiana Shelf hypoxia in the northern Gulf as
528 well as recent studies engendered by the Deepwater Horizon blowout, few studies
529 have addressed the issue of the shelf's influence on open Gulf waters and then
530 generally only in a tangential way. For instance, early studies by Brooks et al. [104],
531 Reid [105], and Todd et al. [106] all pointed to the likelihood of off-shelf transport of
532 methane and radium in the Gulf. Likewise, Trefry and Presley [107] suggested that
533 Mn fluxes from shelf sediments provided a source for 'excess' Mn in deep Gulf of
534 Mexico sediments. Nonetheless, these studies have not been followed up by more
535 detailed surveys or process studies. Surprisingly, TEI distributions in open waters of
536 the Gulf are generally unknown.
537

538 In this report, we have summarized evidence supporting the importance of
539 continental shelves and shelf seas in the oceanic mass balance of TEIs. Furthermore,
540 we have outlined a methodology utilizing ^{228}Ra to more consistently estimate the
541 flux of TEIs from the margins to the open ocean. To improve these estimates, we
542 recommend that GEOTRACES sections place more emphasis on sampling along the
543 margins and that increased consideration be given to completing margin-focused
544 sections, such as that previously proposed for the Gulf of Mexico.

Data accessibility

http://data.bco-dmo.org/jg/dir/BCO/GEOTRACES/NorthAtlanticTransect/

Authors' contributions

All authors contributed to the discussion that formed the basis of this manuscript during the Royal Society workshop on "Quantifying fluxes and processes in trace-metal cycling at ocean boundaries" (Chicheley Hall, UK, December 9-10, 2015). M.A.C. wrote the manuscript with significant written contributions or editorial comments from all authors. M.A.C., P.J.L., M.C.L, and E.Y.K. developed the concept for ^{228}Ra as a TEI shelf flux gauge. V.H. and G.A.C. wrote the introduction. A.M. organized the vast reference list. C.J., A.M.S., P.W.B., W.B.H., H.T., P.S.A., D.P., and F.D. contributed written examples and figures for the review section of the manuscript. All authors gave final approval for publication.

Competing interests

The authors' declare no competing interests.

Funding

This paper would not have been possible without the financial support of a number of national funding agencies (U.S. NSF OCE-1458305 to M.A.C.; Korea NRF-2013R1A1A1058203 to E.Y.K; U.K. NERC NE/G016267/1 to M.C.L and A.M.; U.K. NERC NE/K009532/1 to W.B.H.).

Acknowledgements

We thank Gideon Henderson and the meeting organizers for inviting us to participate in the Royal Society workshop and contribute a paper to the special issue. For their constructive comments on the manuscript the authors thank Editor Micha Rijkenberg, Michiel Rutgers van der Loeff, and one anonymous reviewer. We gratefully acknowledge Francois Primeau for his feedback on derivation of the TEI flux model and Abby Bull of the British Oceanographic Data Centre for her assistance with data mining for the paper.

Literature Cited

1. Simpson JH, Sharples J. Introduction to the Physical and Biological Oceanography of Shelf Seas: Cambridge University Press; 2012.
2. Bourgeois T, Orr JC, Resplandy L, Ethé C, Gehlen M, Bopp L. Coastal-ocean uptake of anthropogenic carbon. Biogeosci Disc. 2016;2016:1-34.
3. Chen C-TA, Borges AV. Reconciling opposing views on carbon cycling in the coastal ocean: Continental shelves as sinks and near-shore ecosystems as sources of atmospheric CO2. Deep Sea Res (Part II: Top Stud Oceanogr). 2009;56(8-10):578-90.
4. Regnier P, Friedlingstein P, Ciais P, Mackenzie FT, Gruber N, Janssens IA, et al. Anthropogenic perturbation of the carbon fluxes from land to ocean. Nature Geo. 2013;6(8):597-607.
5. Olausson E, Cato I, (Eds). Chemistry and biochemistry of estuaries. Chichester: John Wiley & Sons Ltd; 1980. 452 p.
6. Boyle EA, Edmond JM, Sholkovitz ER. Mechanism of iron removal in estuaries. Geochim Cosmochim Acta. 1977;41(9):1313-24.
7. Eckert JM, Sholkovitz ER. Flocculation of iron, aluminum and humates from river water by electrolytes. Geochim Cosmochim Acta. 1976;40(7):847-8.
8. Sholkovitz ER, Copland D. The coagulation, solubility and adsorption properties of Fe, Mn, Cu, Ni, Cd, Co and humic acids in a river water. Geochim Cosmochim Acta. 1981;45(2):181-9.
9. Barnes CE, Cochran JK. Uranium geochemistry in estuarine sediments - controls on removal and release processes. Geochim Cosmochim Acta. 1993;57(3):555-69.
10. Church TM, Sarin MM, Fleisher MQ, Ferdelman TG. Salt marshes: An important coastal sink for dissolved uranium. Geochim Cosmochim Acta. 1996;60(20):3879-87.
11. Andersen MB, Stirling CH, Porcelli D, Halliday AN, Andersson PS, Baskaran M. The tracing of riverine U in Arctic seawater with very precise U-234/U-238 measurements. Earth Planet Sci Lett. 2007;259(1-2):171-85.
12. Elderfield H, Upstillgoddard R, Sholkovitz ER. The rare-earth elements in rivers, estuaries, and coastal seas and their significance to the composition of ocean waters. Geochim Cosmochim Acta. 1990;54(4):971-91.
13. Rousseau TCC, Sonke JE, Chmeleff J, van Beek P, Souhaut M, Boaventura G, et al. Rapid neodymium release to marine waters from lithogenic sediments in the Amazon estuary. Nature Comm. 2015;6.
14. Sholkovitz E, Szymczak R. The estuarine chemistry of rare earth elements: comparison of the Amazon, Fly, Sepik and the Gulf of Papua systems. Earth Planet Sci Lett. 2000;179(2):299-309.
15. Sholkovitz ER, Cochran JK, Carey AE. Laboratory stidues of the diagenesis and mobility of Pu-239, Pu-240 and Cs-137 in nearshore sediments. Geochim Cosmochim Acta. 1983;47(8):1369-79.

16. Carroll J, Falkner KK, Brown ET, Moore WS. The role of the Ganges-Brahmaputra mixing zone in supplying barium and Ra-226 to the Bay of Bengal. Geochim Cosmochim Acta. 1993;57(13):2981-90.
17. Coffey M, Dehairs F, Collette O, Luther G, Church T, Jickells T. The behaviour of dissolved barium in estuaries. Estuar Coast Shelf Sci. 1997;45(1):113-21.
18. Edmond JM, Boyle ED, Drummond D, Grant B, Mislick T. Desorption of barium in the plume of the Zaire (Congo) River. Netherlands J of Sea Res. 1978;12(3-4):324-8.
19. Hanor JS, Chan LH. Non-conservative behaviour of barium during mixing of Mississippi River and Gulf of Mexico waters. Earth Planet Sci Lett. 1977;37(2):242-50.
20. Li YH, Chan LH. Desorption of Ba and Ra-226 from river-borne sediments in the Hudson estuary. Earth Planet Sci Lett. 1979;43(3):343-50.
21. Martin JM, Meybeck M. Elemental mass-balance of material carried by major world rivers. Mar Chem. 1979;7(3):173-206.
22. Burnett WC, Dulaiova H, Stringer C, Peterson R. Submarine groundwater discharge: Its measurement and influence on the coastal zone. J Coast Res. 2006:35-8.
23. Moore WS. Large groundwater inputs to coastal waters revealed by Ra-226 enrichments. Nature. 1996;380(6575):612-4.
24. Moore WS, Sarmiento JL, Key RM. Submarine groundwater discharge revealed by Ra-228 distribution in the upper Atlantic Ocean. Nature Geo. 2008;1(5):309-11.
25. Rodellas V, Garcia-Orellana J, Masque P, Feldman M, Weinstein Y. Submarine groundwater discharge as a major source of nutrients to the Mediterranean Sea. Proc Natl Acad Sci USA. 2015;112(13):3926-30.
26. Kwon EY, Kim G, Primeau F, Moore WS, Cho H-M, DeVries T, et al. Global estimate of submarine groundwater discharge based on an observationally constrained radium isotope model. Geophys Res Lett. 2014;41(23):8438-44.
27. Windom HL, Moore WS, Niencheski LFH, Jahrike RA. Submarine groundwater discharge: A large, previously unrecognized source of dissolved iron to the South Atlantic Ocean. Mar Chem. 2006;102(3-4):252-66.
28. Bone SE, Charette MA, Lamborg CH, Gonneea ME. Has submarine groundwater discharge been overlooked as a source of mercury to coastal waters? Environ Sci Technol. 2007;41(9):3090-5.
29. Trezzi G, Garcia-Orellana J, Santos-Echeandia J, Rodellas V, Garcia-Solsona E, Garcia-Fernandez G, et al. The influence of a metal-enriched mining waste deposit on submarine groundwater discharge to the coastal sea. Mar Chem. 2016;178:35-45.
30. Gonneea ME, Charette MA, Liu Q, Herrera-Silveira JA, Morales-Ojeda SM. Trace element geochemistry of groundwater in a karst subterranean estuary (Yucatan Peninsula, Mexico). Geochim Cosmochim Acta. 2014;132:31-49.
31. Arsouze T, Dutay JC, Lacan F, Jeandel C. Reconstructing the Nd oceanic cycle using a coupled dynamical - biogeochemical model. Biogeosciences. 2009;6(12):2829-46.

664 32. Jeandel C, Oelkers EH. The influence of terrigenous particulate material
665 dissolution on ocean chemistry and global element cycles. Chem Geol.
666 2015;395:50-66.
667 33. Tachikawa K, Athias V, Jeandel C. Neodymium budget in the modern ocean
668 and paleo-oceanographic implications. J Geophys Res:Oceans. 2003;108(C8).
669 34. Abbott AN, Haley BA, McManus J, Reimers CE. The sedimentary flux of
670 dissolved rare earth elements to the ocean. Geochim Cosmochim Acta.
671 2015;154:186-200.
672 35. Blain S, Queguiner B, Armand L, Belviso S, Bombled B, Bopp L, et al. Effect of
673 natural iron fertilization on carbon sequestration in the Southern Ocean.
674 Nature. 2007;446(7139):1070-U1.
675 36. Bowie AR, van der Merwe P, Queroue F, Trull T, Fourquez M, Planchon F, et
676 al. Iron budgets for three distinct biogeochemical sites around the Kerguelen
677 Archipelago (Southern Ocean) during the natural fertilisation study, KEOPS-
678 2. Biogeosciences. 2015;12(14):4421-45.
679 37. Pollard RT, Salter I, Sanders RJ, Lucas MI, Moore CM, Mills RA, et al. Southern
680 Ocean deep-water carbon export enhanced by natural iron fertilization.
681 Nature. 2009;457(7229):577-U81.
682 38. Anderson RF, Mawji E, Cutter GA, Measures CI, Jeandel C. GEOTRACES
683 Changing the Way We Explore Ocean Chemistry. Oceanography.
684 2014;27(1):50-61.
685 39. Anderson RF, Henderson GM. Program update: GEOTRACES—A Global study
686 of the marine biogeochemical cycles of trace elements and their isotopes.
687 Oceanography. 2005;18(3):76-9.
688 40. Plan GS. GEOTRACES: An international study of the marine biogeochemical
689 cycles of traces elements and their isotopes: Scientific Committee in Ocean
690 Research; 2006.
691 41. Mawji E, Schlitzer R, Dodas EM, Abadie C, Abouchami W, Anderson RF, et al.
692 The GEOTRACES Intermediate Data Product 2014. Mar Chem. 2015;177:1-8.
693 42. Glavovic BC, Limburg K, Liu KK, Emeis KC, Thomas H, Kremer H, et al. Living
694 on the Margin in the Anthropocene: engagement arenas for sustainability
695 research and action at the ocean-land interface. Curr Opin Env Sustain.
696 2015;14:232-8.
697 43. McGranahan G, Balk D, Anderson B. The rising tide: assessing the risks of
698 climate change and human settlements in low elevation coastal zones.
699 Environ Urban. 2007;19(1):17-37.
700 44. Small C, Nicholls RJ. A global analysis of human settlement in coastal zones. J
701 Coast Res. 2003;19(3):584-99.
702 45. Boyle EA, Lee J-M, Echegoyen Y, Noble A, Moos S, Carrasco G, et al.
703 Anthropogenic Lead Emission in the Ocean The Evolving Global Experiment.
704 Oceanography. 2014;27(1):69-75.
705 46. Lamborg CH, Hammerschmidt CR, Bowman KL, Swarr GJ, Munson KM,
706 Ohnemus DC, et al. A global ocean inventory of anthropogenic mercury based
707 on water column measurements. Nature. 2014;512(7512):65-+.

47. Bhatia MP, Kujawinski EB, Das SB, Breier CF, Henderson PB, Charette MA. Greenland meltwater as a significant and potentially bioavailable source of iron to the ocean. Nature Geo. 2013;6(4):274-8.
48. Hopwood MJ, Bacon S, Arendt K, Connelly DP, Statham PJ. Glacial meltwater from Greenland is not likely to be an important source of Fe to the North Atlantic. Biogeochemistry. 2015;124(1-3):1-11.
49. Jeandel C. Solid river inputs and ocean margins as critical sources of elements to the oceans. Philos Trans R Soc London, Ser A. 2016;In Press (this issue).
50. Jakobsson M. Hypsometry and volume of the Arctic Ocean and its constituent seas. Geochem Geophys Geosystems. 2002;3.
51. Aagaard K, Carmack EC. The role of sea ice and other freshwater in the arctic circulation. J Geophys Res:Oceans. 1989;94(C10):14485-98.
52. Moore RM. Oceanographic distributions of zinc, cadmium, copper and aluminum in waters of the central Arctic. Geochim Cosmochim Acta. 1981;45(12):2475-82.
53. Ripperger S, Rehkaemper M, Porcelli D, Halliday AN. Cadmium isotope fractionation in seawater - A signature of biological activity. Earth Planet Sci Lett. 2007;261(3-4):670-84.
54. Lambelet M, Rehkaemper M, de Flierdt Tv, Xue Z, Kreissig K, Coles B, et al. Isotopic analysis of Cd in the mixing zone of Siberian rivers with the Arctic Ocean-New constraints on marine Cd cycling and the isotope composition of riverine Cd. Earth Planet Sci Lett. 2013;361:64-73.
55. Roeske T, Bauch D, Van Der Loeff MR, Rabe B. Utility of dissolved barium in distinguishing North American from Eurasian runoff in the Arctic Ocean. Mar Chem. 2012;132:1-14.
56. Thomas H, Shadwick E, Dehairs F, Lansard B, Mucci A, Navez J, et al. Barium and carbon fluxes in the Canadian Arctic Archipelago. J Geophys Res:Oceans. 2011;116.
57. Middag R, de Baar HJW, Laan P, Klunder MB. Fluvial and hydrothermal input of manganese into the Arctic Ocean. Geochim Cosmochim Acta. 2011;75(9):2393-408.
58. McAlister JA, Orians KJ. Dissolved gallium in the Beaufort Sea of the Western Arctic Ocean: A GEOTRACES cruise in the International Polar Year. Mar Chem. 2015;177:101-9.
59. Andersson PS, Porcelli D, Frank M, Bjork G, Dahlqvist R, Gustafsson O. Neodymium isotopes in seawater from the Barents Sea and Fram Strait Arctic-Atlantic gateways. Geochim Cosmochim Acta. 2008;72(12):2854-67.
60. Porcelli D, Andersson PS, Baskaran M, Frank M, Bjork G, Semiletov I. The distribution of neodymium isotopes in Arctic Ocean basins. Geochim Cosmochim Acta. 2009;73(9):2645-59.
61. Dahlqvist RM, Andersson PS, Porcelli D. REE seawater concentrations in the Bering Strait and the Chukchi Sea. Ocean Sciences 2008 Meeting Poster session #0722008.
62. Persson P, Andersson PS, Porcelli D, Semiletov I. The influence of Lena River water inflow and shelf sediment-sea water exchange for the Nd isotopic

composition in the Laptev Sea and Arctic Ocean. European Geosciences Union 2011 Meeting Abstract 1012032011.
63. Alling V, Sanchez-Garcia L, Porcelli D, Pugach S, Vonk JE, van Dongen B, et al. Nonconservative behavior of dissolved organic carbon across the Laptev and East Siberian seas. Global Biogeochem Cycles. 2010;24.
64. Alling V, Porcelli D, Morth CM, Anderson LG, Sanchez-Garcia L, Gustafsson O, et al. Degradation of terrestrial organic carbon, primary production and out-gassing of CO2 in the Laptev and East Siberian Seas as inferred from delta C-13 values of DIC. Geochim Cosmochim Acta. 2012;95:143-59.
65. Portnov A, Smith AJ, Mienert J, Cherkashov G, Rekant P, Semenov P, et al. Offshore permafrost decay and massive seabed methane escape in water depths > 20m at the South Kara Sea shelf. Geophys Res Lett. 2013;40(15):3962-7.
66. Shakhova N, Semiletov I, Salyuk A, Yusupov V, Kosmach D, Gustafsson O. Extensive Methane Venting to the Atmosphere from Sediments of the East Siberian Arctic Shelf. Science. 2010;327(5970):1246-50.
67. Whitmore L, Shiller AM. Dissolved methane in the US GEOTRACES Arctic scetion. Ocean Sciences 2016 Meeting Poster A44A-26832016.
68. Rutgers van der Loeff M, Key RM, Scholten J, Bauch D, Michel A. Ra-228 as a tracer for shelf water in the Arctic Ocean. Deep Sea Res (Part II: Top Stud Oceanogr). 1995;42(6):1533-53.
69. Rutgers van der Loeff M, Cai P, Stimac I, Bauch D, Hanfland C, Roeske T, et al. Shelf-basin exchange times of Arctic surface waters estimated from Th-228/Ra-228 disequilibrium. J Geophys Res:Oceans. 2012;117.
70. Aguilar-Islas AM, Hurst MP, Buck KN, Sohst B, Smith GJ, Lohan MC, et al. Micro- and macronutrients in the southeastern Bering Sea: Insight into iron-replete and iron-depleted regimes. Prog Oceanogr. 2007;73(2):99-126.
71. Elrod VA, Berelson WM, Coale KH, Johnson KS. The flux of iron from continental shelf sediments: A missing source for global budgets. Geophys Res Lett. 2004;31(12):art. no.-L12307.
72. Tyrrell T, Merico A, Waniek JJ, Wong CS, Metzl N, Whitney F. Effect of seafloor depth on phytoplankton blooms in high-nitrate, low-chlorophyll (HNLC) regions. J Geophys Res: Biogeosci. 2005;110(G2).
73. Tagliabue A, Aumont O, Bopp L. The impact of different external sources of iron on the global carbon cycle. Geophys Res Lett. 2014;41(3):920-6.
74. Charette MA, Gonneea ME, Morris PJ, Statham P, Fones G, Planquette H, et al. Radium isotopes as tracers of iron sources fueling a Southern Ocean phytoplankton bloom. Deep Sea Res (Part II: Top Stud Oceanogr). 2007;54(18-20):1989-98.
75. Dulaiova H, Ardelan MV, Henderson PB, Charette MA. Shelf-derived iron inputs drive biological productivity in the southern Drake Passage. Global Biogeochem Cycles. 2009;23.
76. van Beek P, Bourquin M, Reyss JL, Souhaut M, Charette MA, Jeandel C. Radium isotopes to investigate the water mass pathways on the Kerguelen Plateau (Southern Ocean). Deep Sea Res (Part II: Top Stud Oceanogr). 2008;55(5-7):622-37.

77. Boyd PW, Strzepek R, Chiswell S, Chang H, DeBruyn JM, Ellwood M, et al. Microbial control of diatom bloom dynamics in the open ocean. Geophys Res Lett. 2012;39.
78. John SG, Adkins J. The vertical distribution of iron stable isotopes in the North Atlantic near Bermuda. Global Biogeochem Cycles. 2012;26.
79. Labatut M, Lacan F, Pradoux C, Chmeleff J, Radic A, Murray JW, et al. Iron sources and dissolved-particulate interactions in the seawater of the Western Equatorial Pacific, iron isotope perspectives. Global Biogeochem Cycles. 2014;28(10):1044-65.
80. Lacan F, Radic A, Jeandel C, Poitrasson F, Sarthou G, Pradoux C, et al. Measurement of the isotopic composition of dissolved iron in the open ocean. Geophys Res Lett. 2008;35(24):5.
81. Radic A, Lacan F, Murray JW. Iron isotopes in the seawater of the equatorial Pacific Ocean: New constraints for the oceanic iron cycle. Earth Planet Sci Lett. 2011;306(1-2):1-10.
82. Conway TM, Rosenberg AD, Adkins JF, John SG. A new method for precise determination of iron, zinc and cadmium stable isotope ratios in seawater by double-spike mass spectrometry. Anal Chim Acta. 2013;793:44-52.
83. Conway TM, John SG. Quantification of dissolved iron sources to the North Atlantic Ocean. Nature. 2014;511(7508):212-+.
84. Fitzsimmons JN, Carrasco GG, Wu J, Roshan S, Hatta M, Measures CI, et al. Partitioning of dissolved iron and iron isotopes into soluble and colloidal phases along the GA03 GEOTRACES North Atlantic Transect. Deep Sea Res (Part II: Top Stud Oceanogr). 2015;116:130-51.
85. Homoky WB, John SG, Conway TM, Mills RA. Distinct iron isotopic signatures and supply from marine sediment dissolution. Nature Comm. 2013;4:10.
86. Homoky WB, Severmann S, Mills RA, Statham PJ, Fones GR. Pore-fluid Fe isotopes reflect the extent of benthic Fe redox recycling: Evidence from continental shelf and deep-sea sediments. Geology. 2009;37(8):751-4.
87. Homoky WB, Hembury DJ, Hepburn LE, Mills RA, Statham PJ, Fones GR, et al. Iron and manganese diagenesis in deep sea volcanogenic sediments and the origins of pore water colloids. Geochim Cosmochim Acta. 2011;75(17):5032-48.
88. Homoky WB, Weber T, Berelson WM, Conway TM, Henderson GM, van Hulten M, et al. An assessment of oceanic trace element and isotope exchange at the sediment-water boundary. Philos Trans R Soc London, Ser A. 2016;In Press (this issue).
89. Charette MA, Morris PJ, Henderson PB, Moore WS. Radium isotope distributions during the US GEOTRACES North Atlantic cruises. Mar Chem. 2015;177:184-95.
90. Moore WS, Astwood H, Lindstrom C. Radium isotopes in coastal waters on the Amazon shelf. Geochim Cosmochim Acta. 1995;59(20):4285-98.
91. Krest JM, Moore WS, Rama. Ra-226 and Ra-228 in the mixing zones of the Mississippi and Atchafalaya Rivers: indicators of groundwater input. Mar Chem. 1999;64(3):129-52.

92. Moore WS. Inappropriate attempts to use distributions of Ra-228 and Ra-226 in coastal waters to model mixing and advection rates. Cont Shelf Res. 2015;105:95-100.
93. Moore WS. Determining coastal mixing rates using radium isotopes. Cont Shelf Res. 2000;20(15):1993-2007.
94. Saito MA, Moffett JW, DiTullio GR. Cobalt and nickel in the Peru upwelling region: A major flux of labile cobalt utilized as a micronutrient. Global Biogeochem Cycles. 2004;18(4).
95. Bown J, Boye M, Baker A, Duvieilbourg E, Lacan F, Le Moigne F, et al. The biogeochemical cycle of dissolved cobalt in the Atlantic and the Southern Ocean south off the coast of South Africa. Mar Chem. 2011;126(1-4):193-206.
96. Dale AW, Nickelsen L, Scholz F, Hensen C, Oschlies A, Wallmann K. A revised global estimate of dissolved iron fluxes from marine sediments. Global Biogeochem Cycles. 2015;29(5):691-707.
97. Landing WM, Bruland KW. The Contrasting Biogeochemistry of Iron and Manganese in the Pacific-Ocean. Geochim Cosmochim Acta. 1987;51(1):29-43.
98. McManus J, Berelson WM, Severmann S, Johnson KS, Hammond DE, Roy M, et al. Benthic manganese fluxes along the Oregon-California continental shelf and slope. Cont Shelf Res. 2012;43:71-85.
99. Saito MA, Moffett JW. Temporal and spatial variability of cobalt in the Atlantic Ocean. Geochim Cosmochim Acta. 2002;66(11):1943-53.
100. Dulaquais G, Boye M, Rijkenberg MJA, Carton X. Physical and remineralization processes govern the cobalt distribution in the deep western Atlantic Ocean. Biogeosciences. 2014;11(6):1561-80.
101. Powell CF, Baker AR, Jickells TD, Bange HW, Chance RJ, Yodle C. Estimation of the Atmospheric Flux of Nutrients and Trace Metals to the Eastern Tropical North Atlantic Ocean. J Atmos Sci. 2015;72(10):4029-45.
102. Little SH, Vance D, Walker-Brown C, Landing WM. The oceanic mass balance of copper and zinc isotopes, investigated by analysis of their inputs, and outputs to ferromanganese oxide sediments. Geochim Cosmochim Acta. 2014;125:673-93.
103. Tanaka T, Yasuda I, Kuma K, Nishioka J. Vertical turbulent iron flux sustains the Green Belt along the shelf break in the southeastern Bering Sea. Geophys Res Lett. 2012;39.
104. Brooks JM, Reid DF, Bernard BB. Methane in the upper water column of the northwestern Gulf of Mexico. J Geophys Res:Oceans. 1981;86(NC11):1029-40.
105. Reid DF. Radium variability produced by shelf-water transport and mixing in the western Gulf of Mexico. Deep Sea Res (Part I: Oceanogr Res Papers). 1984;31(12):1501-10.
106. Todd JF, Wong GTF, Reid DF. The geochemistries of Po-210 and Pb-210 in waters overlying and within the Orca Basin, Gulf of Mexico. Deep Sea Res (Part I: Oceanogr Res Papers). 1986;33(10):1293-306.
107. Trefry JH, Presley BJ. Manganese fluxes from Mississippi Delta sediments. Geochim Cosmochim Acta. 1982;46(10):1715-26.

108. Sholkovitz ER. The geochemistry of rare-earth elements in the Amazon River estuary. Geochim Cosmochim Acta. 1993;57(10):2181-90.

Tables

Table 1. Western North Atlantic Ocean margin TEI flux estimates derived from shelf ^{228}Ra inputs (14.3 ± 1.9 x 10^{22} atoms/y; 0-70°N) and $\Delta TEI/\Delta^{228}Ra$ ratios. The integrated shelf area used to normalize the basin-scale fluxes was 2.5 x 10^{12} m^2.

	dCo	dFe	dMn	dZn
TEI/^{228}Ra (x 10^{-6} nmol/atom)	1.0	2.7	3.8	11
TEI Flux (x 10^{8} mol/y)	1.4	3.9	5.4	16
TEI Flux (µmol/m^2/y)	56	160	220	630

Figures

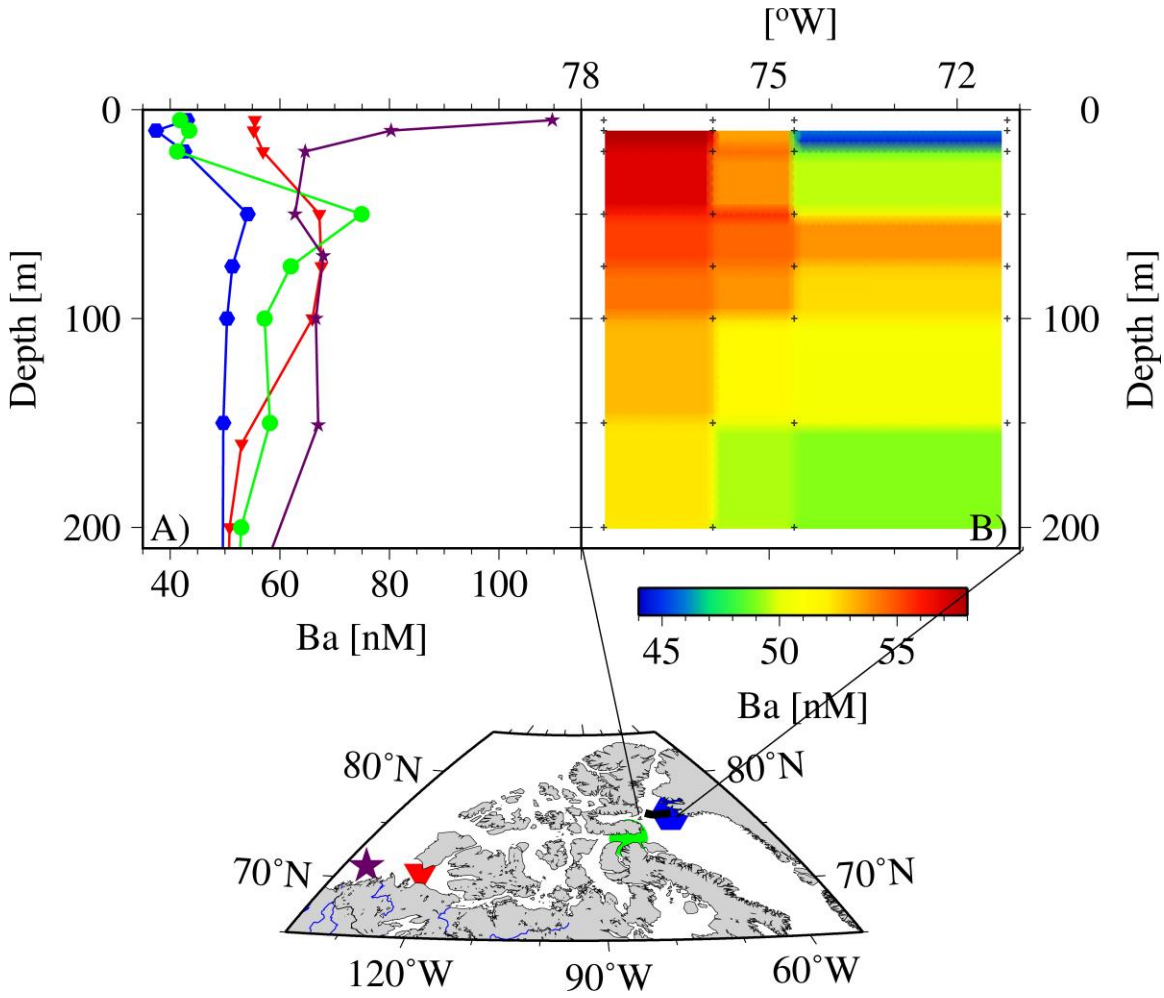

Figure 1. Dissolved Ba concentrations observed in the Canadian Arctic Archipelago during the Canadian CFL-IPY-GEOTRACES program in 2007-2008. A) Profiles of four selected stations across the Archipelago. The easternmost station (blue symbols) is under the influence of northward flowing North Atlantic waters, which reveal substantially lower Ba concentrations than waters sampled at stations within the Archipelago. The westernmost station (purple stars) near the Horton River estuary depicts the riverine surface source of Ba. In Archipelagic waters (green circles), Ba displays a subsurface maximum, which in turn can be used to trace the eastward transport of waters through the Archipelago (redrawn after Thomas et al. [56]). B) Ba contour section across the head of Baffin Bay, approximately along 76° N, as indicated by the black line in the inserted map in A). The easternmost station is identical with the one shown in A) (blue symbols).

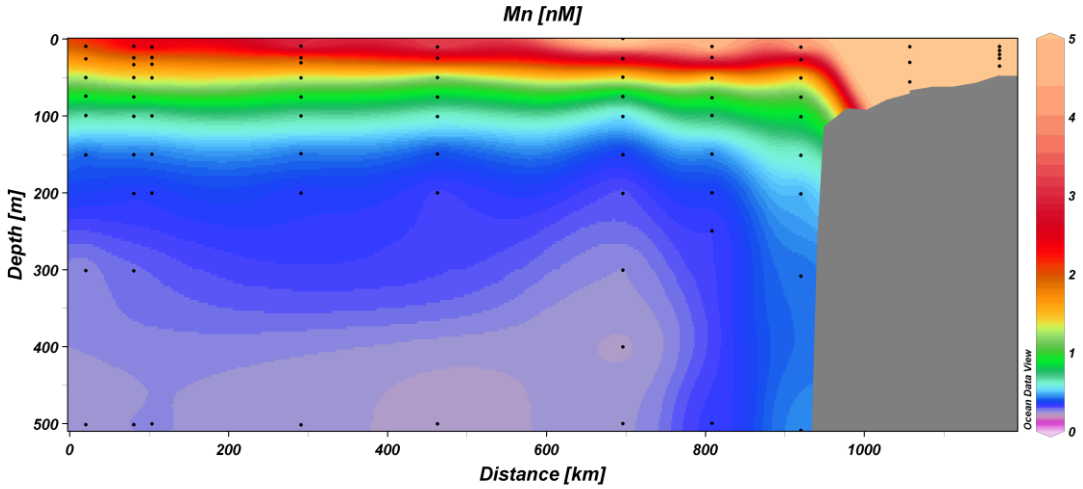

Figure 2. Dissolved Mn (nM) concentrations in the upper 500 m of the Laptev Sea illustrating the strong Mn source over the shelf and its subsequent transport toward the central Arctic basin (Middag et al. [57]).

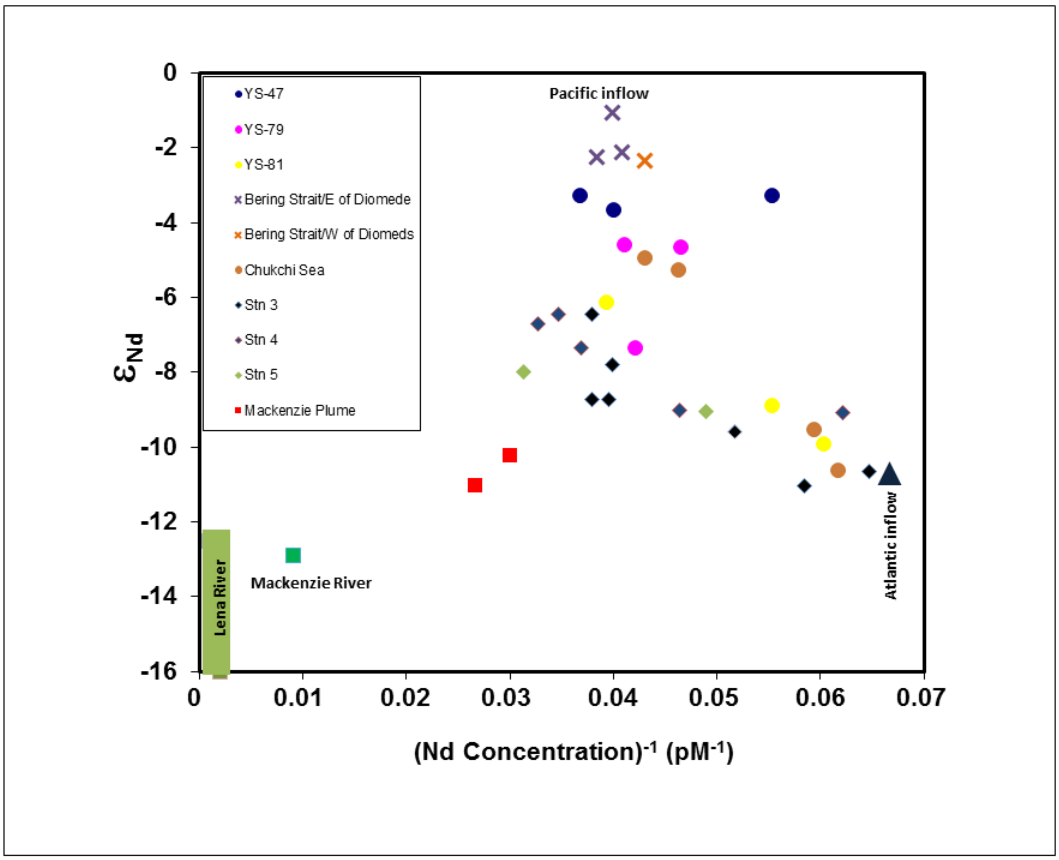

Figure 3. Nd concentration and isotope data for Arctic Ocean waters. The isotope ratios of waters flowing from the Pacific decrease during passage through the Bering Sea before entering the Chukchi Sea in the Arctic due to interaction with shelf sediments (Dahlqvist et al. [61]).

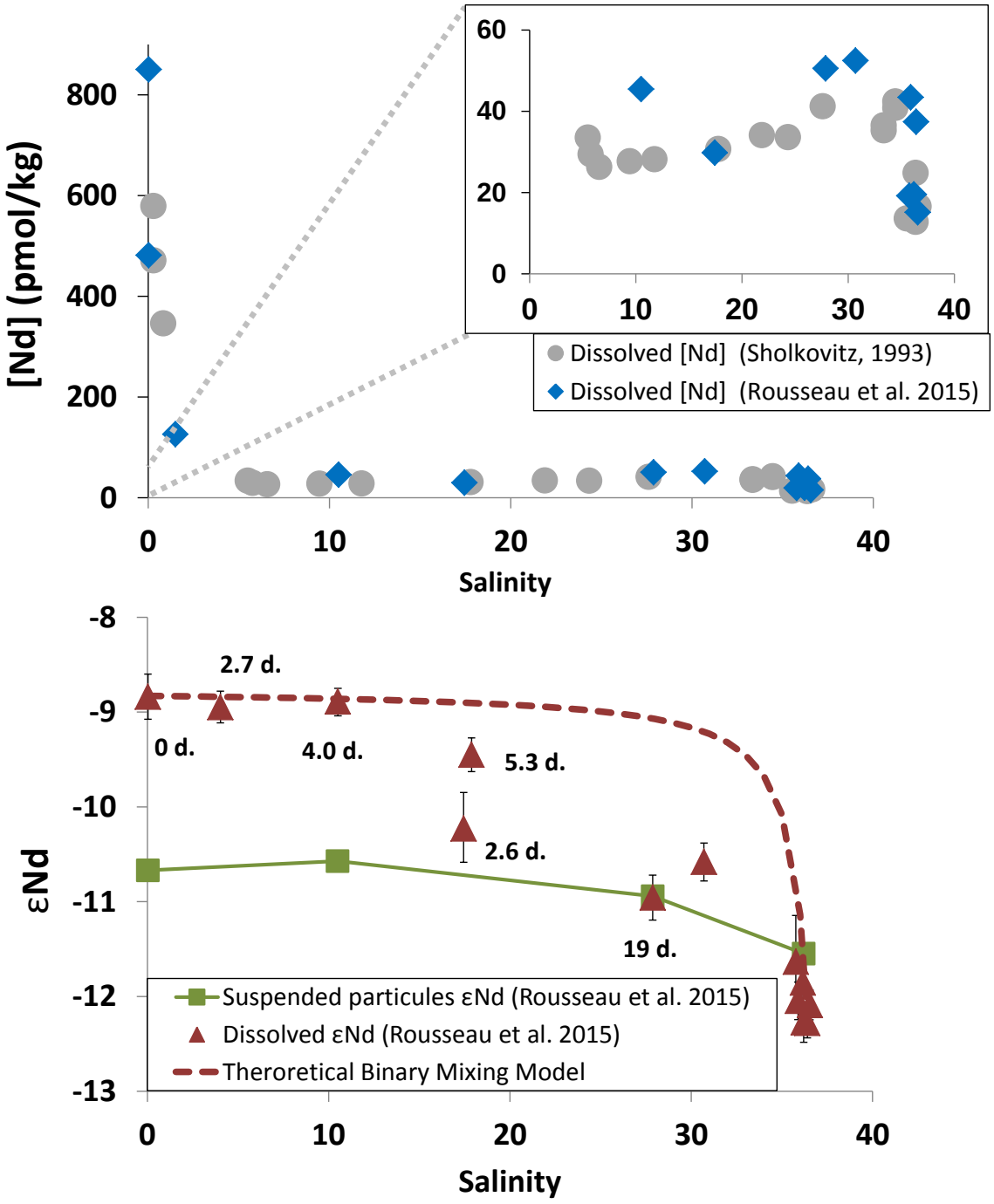

926
927
928 Figure 4. *Upper panel:* Amazon estuary [Nd] from Sholkovitz [108] (grey circles) and
929 Rousseau et al. [13] (blue diamonds) are reported against the salinity gradient.
930 *Lower panel:* Amazon estuary dissolved (red triangles), particulate (green squares)
931 εNd and radium-derived water mass ages (in days) are reported against the salinity
932 gradient.

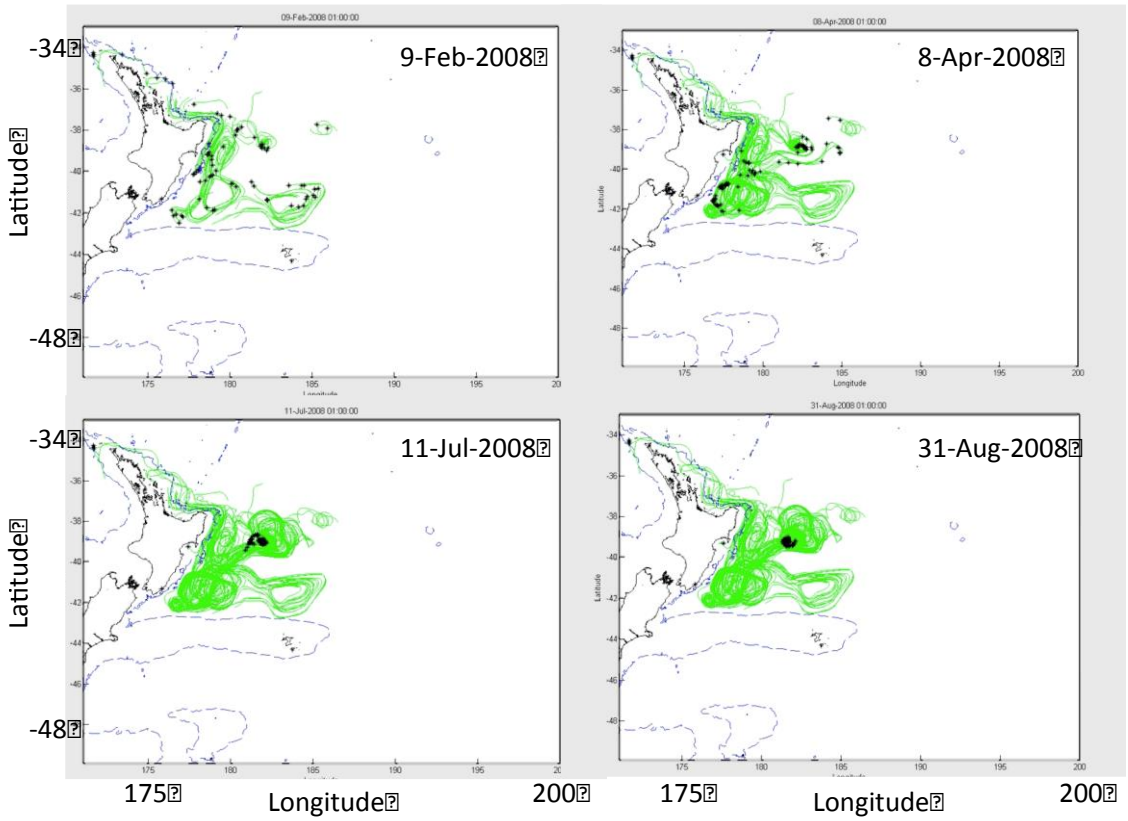

933
934
935 Figure 5. Particle trajectories (green lines) from an altimetry model designed to
936 investigate the origin of water masses within a counterclockwise eddy studied as
937 part of the GEOTRACES FeCycle process study (Boyd et al. [77]). Model snapshots
938 are from (clockwise starting at top left) 9 Feb, 8 April, 11 July and 31 Aug 2008. The
939 particles (black) traverse the waters on and across the 200 m deep shelf break (blue
940 contours) adjacent to the eastern seaboard of the northern island of New Zealand.

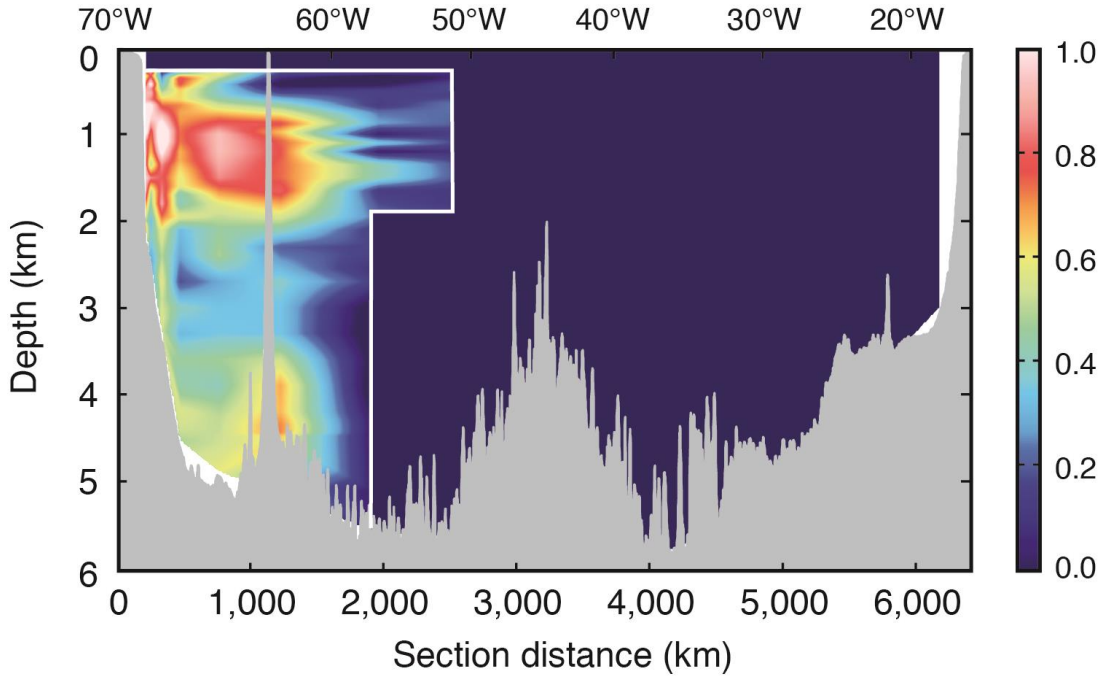

941
942

943 Figure 6. Fraction of water column Fe associated with input from oxygenated
944 sediments along the North Atlantic margin (from Conway and John [83]).

945

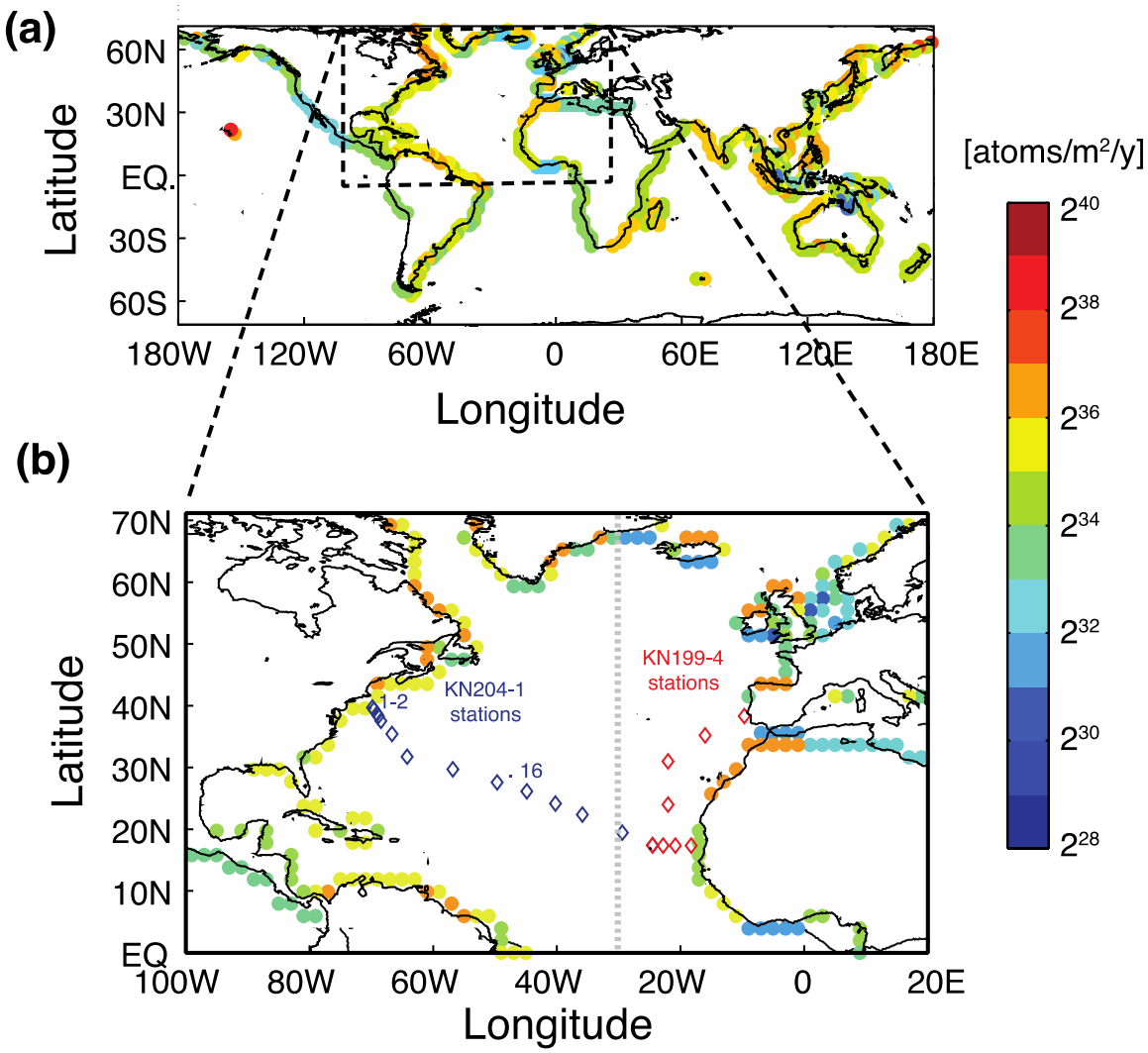

946

947 Figure 7. Model derived shelf ^{228}Ra flux (units are log base (2) atoms m^{-2} y^{-1}) from
948 the model of Kwon et al. [26]. Also shown in (b) are the U.S. GEOTRACES GA03
949 cruise stations (diamonds). The dashed line in (b) is the boundary between the
950 eastern and western Atlantic margins. The innermost coastal and central Atlantic
951 stations were used to derive the ΔTEI/Δ^{228}Ra averages.

952

953

954

955

956

957